Special Feature: Nanostructured Materials

Research Report

Synthesis and Characterization of Microstructure-controlled Carbon Nanotubes

Atsuto Okamoto, Itaru Gunjishima, Takashi Inoue, Riichiro Ohta and Koichi Nishikawa

Report received on July 30, 2011

ABSTRACT Vertically aligned carbon nanotubes (V-CNTs) with controlled diameter, and nitrogen-containing CNTs (NCNTs) were prepared by a catalytic chemical vapor deposition method using highly active and size-classified nanoparticles, and a nitrogenation process with pretreatment by ultraviolet light irradiation, respectively. We present the thermal and electrical conduction properties of V-CNTs, the chemical bonding states of NCNTs, and the electrical conductivity of CNT yarns spun from these. The thermal diffusivity of V-CNTs was ca. 5×10^{-5} $m^2 \cdot s^{-1}$, which is in the same order as that for isotropic graphite. The electrical resistance of the V-CNTs also shows a $T^{-1/4}$ temperature dependence, which implies that the conduction of electrons is dominated by a three-dimensional Mott variable range hopping mechanism. The reduction in the electrical conductivity of NCNT yarns compared to that of CNT yarns is attributed to the formation of chemical bonding sites such as pyridinic and pyrrolic sites and a reduction of crystallinity via the nitrogenation process.

KEYWORDS Carbon Nanotubes, Nanoparticles, Nitrogen, Yarns, Vertically Aligned, Diameter-controlled, Chemical Vapor Deposition, Thermal Diffusivity, Electrical Conductivity

1. Introduction

Carbon nanotubes (CNTs)[1] are one of the most promising materials in nanotechnology applications, because it has been theoretically predicted[2-4] and experimentally confirmed that individual CNTs have high thermal conductivity[5] and low resistivity,[6] similar to those of diamond and copper. The properties of CNTs are strongly dependent on factors such as diameter, chirality, growth orientation, dopant site, defects, and number density.[2,7] Therefore, nanotechnology applications of CNTs require control of the CNT microstructure. For instance, it has been demonstrated in various studies that the use of diameter-controlled and liquid-phase synthesized nanoparticles (NPs) as catalysts is very useful to control the microstructure of CNTs.[8,9] In this paper, the term "microstructure" is used to refer to the diameter, wall number, chemical bonding sites, and vertical alignment of CNTs.

Vertically aligned CNTs (V-CNTs) have been expected to exhibit extraordinary thermal and electrical conduction properties[10] or be used as a starting material for the production of yarns with high tensile strength.[11] There have been a number of reports on V-CNT formation using thermal or plasma-enhanced catalytic chemical vapor deposition (CCVD) methods.[12,13] The synthesis of millimeter-scale length V-CNTs was easily achieved by water (H_2O)-assisted thermal CCVD, the so-called "supergrowth" method.[14] However, little has been reported regarding the simultaneous pursuit of diameter control and vertical alignment of CNTs using NPs to date.

The significant point to be clarified here is whether the properties of 'bulk CNTs' such as V-CNTs and CNT yarns useful in practical applications are comparable to those of the individual CNTs. Although much research has been conducted on the applications of V-CNTs and CNT yarns, the question of how to realize the intrinsic and superior properties of individual CNTs in each application is still open. Therefore, with respect to the applications, it is of significant importance to optimize the properties of bulk CNTs as well as those of individual CNTs. However, there have only been several experimental studies on the thermal[15] and electrical conductivity[16,17]

of V-CNTs grown by the supergrowth or other methods.

In order to gain insight into the benefit of V-CNTs, we firstly examined the formation of vertically aligned and diameter-controlled CNTs from highly active and size-classified NP catalysts prepared by a liquid-phase process.[18-22] Secondly, we clarified the thermal and electrical properties of V-CNTs.[23] Nitrogen-containing CNTs (NCNTs) were then prepared by a nitrogenation process, and the chemical bonding sites of the NCNTs and the electrical conductivity of NCNTs yarns were experimentally evaluated.[24]

2. Experimental

2. 1 Preparation of Catalyst and Substrate

A schematic flow of the CNT growth process is shown in **Fig. 1**. Iron (Fe)-oxygen (O), Fe-vanadium (V)-O, and Fe-titanium (Ti)-O NPs stabilized by oleic acid/oleylamine were prepared by a reduction method using iron(III) acetylacetonate ($Fe(acac)_3$), $VO(acac)_2$, and $TiO(acac)_2$ as metal precursors, respectively.[18-20,25] The as-synthesized NPs can be easily dispersed in hexane. The centrifugal classification of NPs[21,22] is facilitated by fractional precipitation through the sequential addition of ethanol to a hexane solution of NPs. The resultant precipitation was redispersed in hexane. The supernatant solution was also centrifuged under the same conditions, and the subsequent fractionated NPs were redispersed in hexane. Hexane dispersion of each fractionated NP was obtained by repeating the process. The NPs were supported on a 10×10 mm^2 silicon (Si)/mesoporous silica (MPS) substrate by dip-coating. Details of the Si/MPS preparation have been described elsewhere.[26] The concentration of the NP solution was controlled for the self-assembled monolayer deposition of NPs. The surfactants on the NPs (Fig. 1) were finally removed by a 10 min plasma pretreatment to improve the catalytic activity of the NPs.

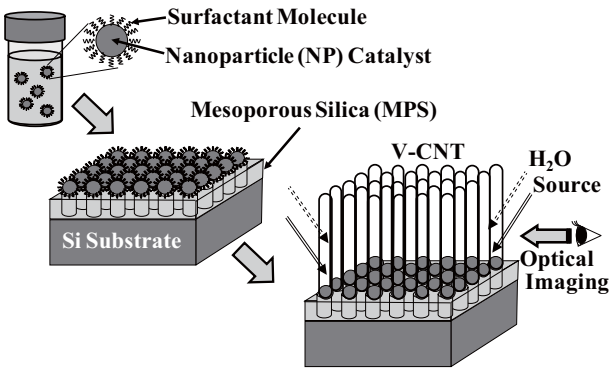

Fig. 1 Schematic flow for the CNT growth process.

2. 2 Growth and Nitrogenation of CNTs

V-CNTs were grown on Si/MPS substrates by a CCVD method using Fe-O, Fe-V-O, and Fe-Ti-O NPs as catalysts, under constant gas flow of C_2H_2 as a source, H_2 or Ar/H_2 as carrier gases, and a small amount of H_2O as a growth-promoting agent. The temperature and total gas pressure were maintained at 700−900°C and 267 Pa during the growth, respectively.

Vertically aligned NCNTs (V-NCNTs) were prepared from pristine V-CNTs by ultraviolet light (UV) irradiation and subsequent nitrogenation with ammonia gas (NH_3), which has been described elsewhere.[24] CNTs oxidized by UV irradiation are referred to here as OCNTs. V-NCNTs without the oxidation treatment were prepared as a reference sample. Already-spun CNT yarns were nitrogenated to produce NCNT yarns.

2. 3 Characterization of NPs and CNTs

The arrangement of NPs on the substrate prior to the CNT growth was observed by field emission scanning electron microscopy (FE-SEM). The composition of the NPs was determined using inductively coupled plasma atomic emission spectrometry (ICP-AES).

The height and morphology of the V-CNTs were measured using FE-SEM and optical observation of the cross-sectional surface. Furthermore, in situ optical imaging (Fig. 1) enabled direct measurement of the growth height and growth rate, which was calculated from the height and sampling time.[27] Feedback control of the growth rate was conducted with reference to the measured growth rate trend by changing growth parameters such as the growth temperature, pressure and gas flow rate.[28] The bulk density of V-CNTs was estimated from the difference in the volume and mass before and after growth. The mean diameters of the NPs and CNTs were measured using transmission electron microscopy (TEM), and are denoted by d_{NP} and d_{CNT}, respectively. For the preparation of TEM samples, CNTs were removed from the substrate, dispersed in ethanol and then dropped on TEM grids and dried under vacuum. The

crystallinity of V-CNTs was examined by TEM and Raman spectroscopy using a laser excitation energy of 5.14 eV.

The thermal diffusivity of the V-CNTs was evaluated by the laser flash method at room temperature in air. The electrical resistance of the V-CNTs was measured using the direct-current four-terminal method at temperatures from 7 to 270 K. The experimental details have been described elsewhere.[15,23]

Nitrogen incorporation into the CNTs was examined by X-ray photoelectron spectroscopy (XPS) composition analysis. The chemical bonding states of NCNTs and OCNTs were assigned according to Fourier transform infrared spectroscopy (FTIR) analysis. The electrical conductivity of CNT yarn and NCNT yarn was compared by nitrogenation of the same CNT yarn.[24]

3. Results and Discussion

3. 1 Growth of V-CNTs from Highly Active NPs

Figure 2 shows FE-SEM images of Fe-O, Fe-V-O (V: 10 mol%), and Fe-Ti-O (Ti: 10 mol%) NPs on substrates after removal of surfactants by plasma treatment and cross-sectional FE-SEM images of CNTs grown from the NPs for 10 min. V-CNTs were grown only from Fe-V-O and Fe-Ti-O NPs, whereas the Fe-O NPs resulted in the growth of a small amount of random CNTs with unaligned morphology with respect to the substrate. This is because Fe-V-O and Fe-Ti-O NPs are more highly active toward the production of V-CNTs than Fe-O NPs.[18-20]

V-CNTs with an outer mean diameter of 4.3 ± 0.7 nm were grown from the Fe-Ti-O NPs (d_{NP} = 3.8 ± 0.6 nm), and were mainly double- and triple-walled (single: 2%, double: 43%, triple: 50%, quadruple: 5%).[18] V-CNTs with d_{CNT} = 3.7 ± 0.6 nm were grown from the Fe-V-O NPs (d_{NP} = 3.1 ± 0.5 nm); the percentages of single-, double- and triple-walled CNTs were 14, 74 and 12, respectively.[19] **Figure 3** summarizes the relationship between the diameters of the NPs and CNTs in the present study together with other data.[8,9,18,19,21,29-33] V-CNTs with diameters almost identical to that of the initial NPs were grown with a relatively smaller standard deviation in a relatively smaller diameter range, compared to the V-CNTs grown from gas-phase synthesized NPs reported in other studies.[32,33] In particular, both the use of centrifugally classified NPs (d_{NP} = 2.8 ± 0.4 nm) and optimization of the growth temperatures were found to be effective for control of the CNT diameter (d_{CNT} = 3.1 ± 0.5 nm).[21,22]

The V-CNT growth height after 10 min using Fe-Ti-O (Ti: 20 mol%) NPs and a small amount of H_2O was three times larger than typical growth without H_2O addition.[23] H_2O vapor is known to act as a protective agent against amorphous carbon coating on catalyst particles, and thus the suitable addition of H_2O vapor should enhance and maintain the activity of the catalyst.[14] The time evolution of the V-CNT growth

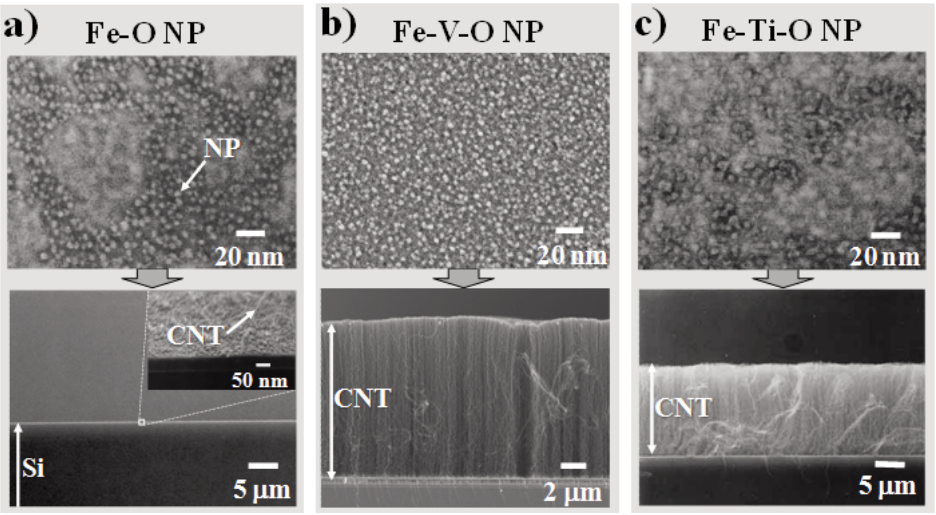

Fig. 2 FE-SEM images of a) Fe-O, b) Fe-V-O, and c) Fe-Ti-O NPs on substrates after removal of surfactants by plasma treatment, and cross-sectional images of grown CNTs. Inset shows an inclined FE-SEM image in which a few CNTs were observed.

height was measured with an in situ optical imaging system (**Fig. 4**).[27,28] The length and bulk density of V-CNTs grown at 700°C for approximately 60 min were in the range of 0.75−1.22 mm and 20−33 kg·m^{-3}, respectively (**Table 1**).

The percentage of the total number of single-, double-, triple-, and quadruple-walled CNTs in the grown CNTs, and the mean outer and inner diameters of V-CNTs grown without H_2O were measured by TEM (**Fig. 5**) as ca. 90%, 5.9 ± 1.5 and 4.2 ± 0.9 nm, respectively, whereas those of the H_2O-assisted V-CNTs were ca. 90%, 5.6 ± 1.1 and 4.0 ± 0.8 nm, respectively. Furthermore, the D band to G band Raman intensity ratio (I_D/I_G) of the H_2O-assisted CNTs was 0.77, while that of the CNTs grown without H_2O

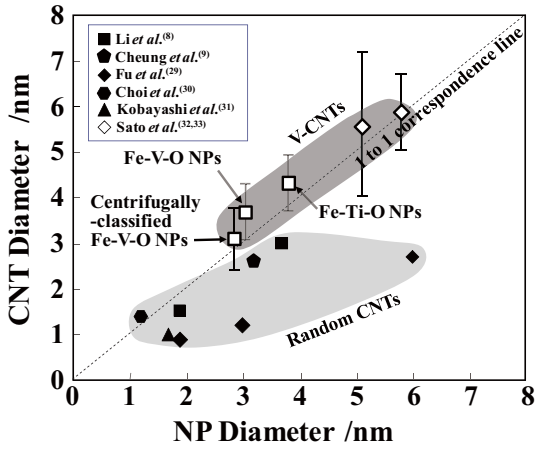

Fig. 3 Relationship between NP and CNT diameters in the present study and other studies.[8,9,18,19,21,29-33] The dashed line indicates the one to one correspondence between the diameters of NPs and CNTs. The solid and open polygons denote random CNTs and V-CNTs, respectively. The error bars, which are shown only in the case of V-CNTs, indicate the standard deviation of each mean diameter.

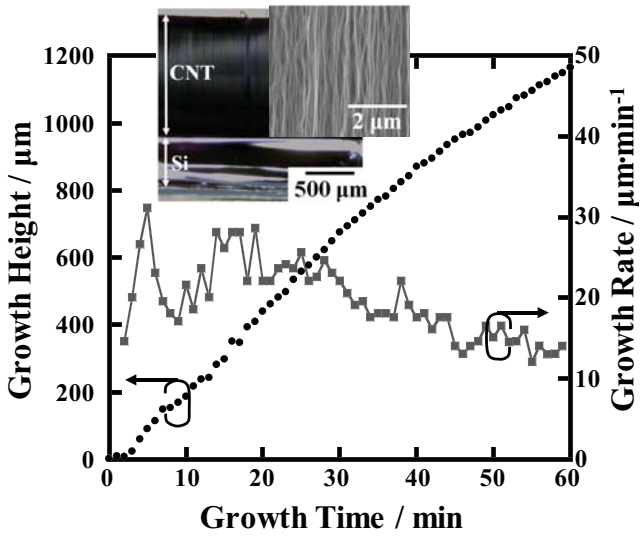

Fig. 4 Time evolution of the growth height and rate measured by in situ optical imaging.[27,28] The inset shows a cross-sectional optical image of as-grown V-CNT on Si/MPS substrate with a typical SEM image of the center area of a V-CNT.

Table 1 Thermal diffusivities of as-grown V-CNTs, isotropic graphite[34] and the supergrowth SWNTs[15] measured by the laser flash method.

Sample	Length (mm)	Density (kg·m^{-3})	Thermal Diffusivity (m^2·s^{-1})
#1	0.75	22.8	5.1×10^{-5}
#2	0.91	19.6	3.6×10^{-5}
#3	1.09	26.1	5.5×10^{-5}
#4	1.22	32.8	6.3×10^{-5}
Isotropic Graphite [34]			ca. 1.0×10^{-4}
Supergrowth SWNTs (as-grown, solid) [15]			$0.75–1.0 \times 10^{-4}$

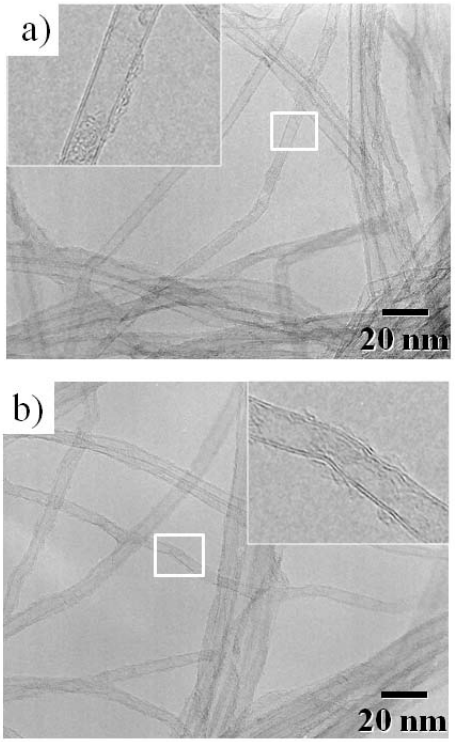

Fig. 5 Typical TEM images of V-CNTs, synthesized a) with and b) without H_2O addition.

was 0.63. There was no significant difference between the two specimens; therefore, H_2O-assisted growth was found to have no influence on the microstructure of the V-CNTs grown in our system. In addition, the I_D/I_G at each measurement point corresponding to the initial, intermediate, and final growth stages was the same. Thus, a small amount of H_2O addition had no effect on the crystallinity of the V-CNTs during growth. Therefore, in the present work, we analyzed the thermal and electrical properties of H_2O-assisted V-CNTs.

3. 2 Thermal and Electrical Properties of V-CNTs

Table 1 presents the thermal diffusivity for various V-CNTs; that for the V-CNTs grown in the present study were from 3.6×10^{-5} to 6.3×10^{-5} $m^2 \cdot s^{-1}$, which is of the same order as isotropic graphite[34] and the supergrowth single-walled CNTs (SWNTs).[15] The thermal conductivity of V-CNTs was estimated to be approximately 1 $W \cdot m^{-1} \cdot K^{-1}$ using the specific heat capacity for graphite (710 $J \cdot kg^{-1} \cdot K^{-1}$) and the bulk density of V-CNTs (Table 1). Low thermal diffusivity of V-CNTs may be caused by low crystallinity (I_D/I_G: ca. 1) and thermal resistance induced by a large number of contacts between CNTs on a 1 mm long CNT.

Figure 6 shows the temperature dependence of the normalized electrical resistance of CNTs, measured both parallel ($R_{\parallel}$) and perpendicular ($R_{\perp}$) to the tube longitudinal axis. The resistance in both directions was increased with decreasing temperature. The temperature dependence of electrical resistance is characteristic of semiconductors, which is in agreement with previous reports.[16,35] The anisotropy ($R_{\perp}/R_{\parallel}$) was gradually increased with decreasing temperature and became pronounced below 15 K, as shown in the inset of Fig. 6. V-CNTs have a large number of intertube and interbundle contacts, and the anisotropy indicates that significant scattering may occur at the contacts as a result of intertube energy barriers. At low temperature T, when the barrier is greater than the thermal energy (k_BT, where k_B is Boltzmann's constant), a localized electron on the CNT is unlikely to hop across a barrier. The marked increase in the anisotropy at low T reflects differences in the perpendicular and parallel hopping rates. The phonon-induced tunneling phenomenon between the localized states can be explained using Mott's law.[36] The logarithmic plots of resistance versus $T^{-1/4}$ shown in **Fig. 7** are linear (dotted lines), which implies that the electronic conduction is mainly dominated by Mott variable range hopping (VRH) in 3D.[16,37-39] The prepared V-CNTs have intertube and interbundle contacts and low thermal diffusivity; therefore, 3D VRH may occur between localized states linked to defects in the tubes and tube contacts.

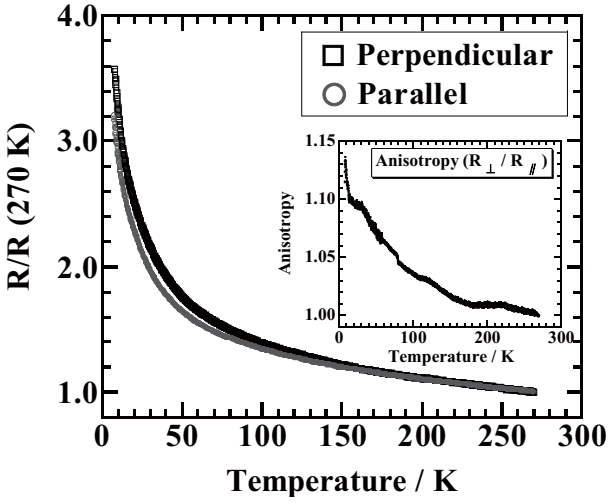

Fig. 6 Temperature dependence of the normalized electrical resistance of CNTs, both perpendicular (□) and parallel (○) to the tube longitudinal axis. The inset shows the temperature dependence of anisotropy ($R_{\perp}/R_{\parallel}$).

3. 3 Nitrogen Incorporation into CNTs and Conductive Properties of CNT Yarns

Figure 8(a) shows a schematic of the process flow for CNT synthesis with XPS results for the C/N/O

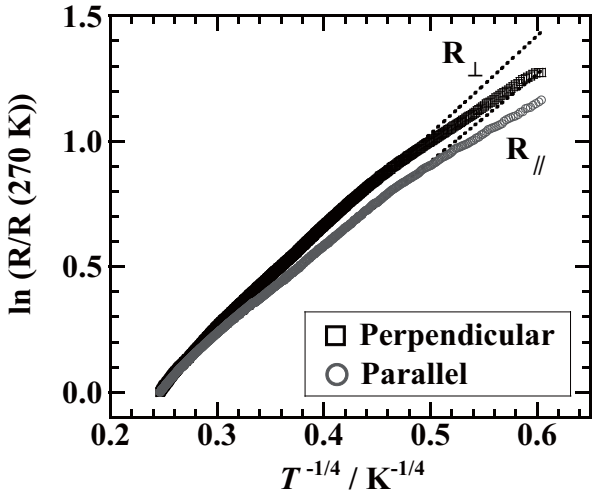

Fig. 7 Logarithmic plot of normalized electrical resistance (ln(R/R (270 K))) versus $T^{-1/4}$ for specimens both perpendicular (□) and parallel (○) to the tube axis.

atomic ratios. Nitrogen is effectively incorporated in CNTs via UV irradiation prior to nitrogenation. The O 1s spectrum of OCNTs was composed of two peaks at ca. 532.0 (O1) and 533.5 eV (O2) that have been assigned to C=O[40] and C−O,[40] respectively (Fig. 8(b)). On the other hand, the decrease in the intensity of these peaks in the NCNTs spectrum indicates that the oxygen-containing functional groups were decreased after nitrogenation. The N 1s spectrum of V-NCNTs consisted of four peaks at ca. 398.3 (N1), 399.7 (N2), 401.0 (N3), and 403.9 eV (N4) (Fig. 8(c)), which were assigned to (N1) pyridinic,[41,42] (N2) pyrrolic,[41] and (N3) quaternary sites,[41,42] and (N4) oxides or shake-up satellites originated from π bonds, respectively.

Figure 9 shows the FTIR difference spectra for OCNTs and NCNTs obtained by subtraction of the IR spectrum for pristine CNTs. The bands at around (I) 1000–1200, (II) 1500–1600, (III) 1600–1700, and (IV) 3000–3500 cm^{-1} in the OCNT spectrum have been assigned to (I) υC−O−C, (II) IR-activated υC=C, (III) υC=O, and (IV) υO−H, respectively.[43] After nitrogenation, bands (III) and (IV) disappeared and the intensity of the band II shoulder at around 1500–1580 cm^{-1}, which is close to the previously reported band assigned to the heteroaromatic ring of graphitic carbon nitride,[44] was increased. The decrease of band I after nitrogenation was relatively small; therefore, the ether groups may be less reactive toward NH_3 than the C=O and C−OH groups. The peaks related to C≡N and N−H groups, which are generally detected at around 2200–2300 and 3000–3500 cm^{-1}, respectively, were not observed.

On the basis of the XPS and FTIR studies, the oxygen-containing functional groups were expected to react with NH_3 to introduce nitrogen covalently as hetero atoms in the aromatic rings composing the tube framework, mostly at pyridinic and pyrrolic sites rather than at quaternary sites. The cylindrical structure was preserved even after nitrogenation, as confirmed by TEM, although disordering of the tube structure was promoted as indicated by the increase in the intensity ratio of I_D/I_G (Raman spectra) from 1.0 to 1.4.

The electrical conductivity of the CNT yarn with a diameter of ca. 10 μm was 4.2×10^4 S m^{-1} and was decreased to 2.8×10^4 S m^{-1} via the nitrogenation process, which contrasts with the increase of electrical conductivity for nitrogen doping by direct synthesis routes reported previously,[45,46] one of which showed the peak for quaternary sites as the most intense in the N 1s spectrum.[46] We assume that the decreased electrical conductivity in the present work is caused by a more predominant influence of disordering in the tube structure rather than by incorporated nitrogen.

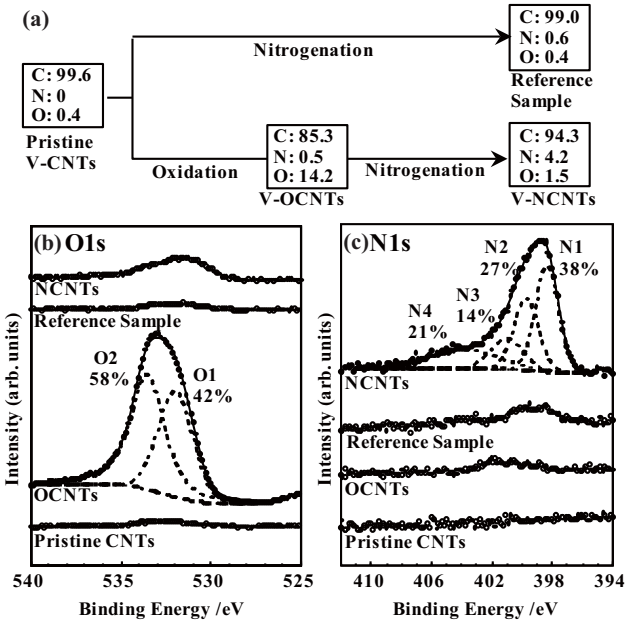

Fig. 8 (a) Schematic representation of the process flow for CNT synthesis, XPS atomic ratios C/N/O, and XPS (b) O 1s and (c) N 1s spectra of obtained samples. Ratios of the peak areas are also shown.

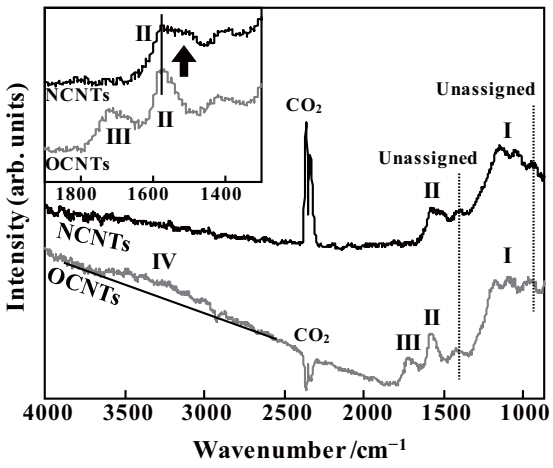

Fig. 9 FTIR difference spectra for OCNTs and NCNTs obtained by subtraction of the IR spectrum for pristine V-CNTs. The insert shows the same spectra in which the wavenumber region around bands II and III was enlarged to clearly show the decrease of band III and increase of the band II shoulder, as indicated by the arrow.

Incorporation of nitrogen with lower concentrations may cause less disordering and possibly enhance the electrical conductivity, as discussed in the previous report.[47] Otherwise, the nitrogen incorporated at pyridinic and pyrrolic sites would have no effect to increase the electrical conductivity, unlike nitrogen incorporation at quaternary sites. However, the catalytic activity of pyridinic sites[48] and a vertically aligned morphology with relative high surface area could be beneficial for other applications.

4. Conclusions

V-CNTs composed of diameter-controlled CNTs were synthesized by a CCVD method using highly active and size-classified Fe-V-O and Fe-Ti-O NPs as catalysts. The thermal diffusivity of the V-CNTs was of the same order as that of isotropic graphite and the estimated thermal conductivity was lower than that of an individual CNT reported previously.[5] The temperature dependence of electrical resistance is characteristic of semiconductors and the anisotropy ($R_{\perp}/R_{\parallel}$) gradually increases with decreasing temperature. The low thermal diffusivity and electrical properties of V-CNTs suggest that 3D Mott VRH may occur between localized states linked to defects in the tubes and intertube contacts. Cylindrical NCNTs with vertically aligned morphology were successfully prepared by a solventless nitrogenation process with UV pretreatment. Nitrogen atoms occupied mostly pyridinic and pyrrolic sites of the CNTs and the crystallinity and electrical conductivity were reduced via the nitrogenation process.

Acknowledgements

We would like to thank our collaborators and co-authors on recent papers who contributed to the synthesis of iron nanoparticles and characterization of carbon nanotubes, including: Dr. S. Yamamuro, Prof. K. Sumiyama and Prof. M. Tanemura (Nagoya Institute of Technology), Dr. M. Akoshima and Dr. T. Baba (AIST), Dr. H. Miyagawa, Dr. T. Nakano and Prof. G. Oomi (Kyushu University), Mr. T. Shimazu, Dr. M. Siry and Dr. H. Oshima (DENSO CORPORATION). We received the cooperation of our colleagues at Toyota Central R&D Labs: Ms. Y. Kumai and Dr. S. Inagaki (preparation of MPS films), Mr. H. Kadoura and Mr. J. Seki (FE-SEM), Mr. N.Suzuki, and Mr. Y. Akimoto (TEM), Mr. Y. Kawai (ICP-AES), Mr. E. Sudo (Raman spectroscopy and FTIR), Ms. N. Takahashi (XPS), Ms. Y. Morimoto and Ms. K. Watanabe (assistance in all experiments), Mr. W. Yamazaki (installation and maintenance of incidental facilities), and Mr. Y. Kimoto, Mr. Y. Miyachi, Dr. M. Toyama, Mr. K. Shinozaki, Mr. T. Hatanaka and Dr. K. Takatori for fruitful discussions. Finally, the authors would like to thank Elsevier Ltd.[21,23] and the Royal Society of Chemistry[24] for their permission to reproduce this paper.

References

(1) Iijima, S., “Helical Microtubules of Graphitic Carbon”, *Nature*, Vol.354, No.6348 (1991), pp.56-58.
(2) Saito, R., Dresselhaus, G. and Dresselhaus, M. S., *Physical Properties of Carbon Nanotubes* (1998), Imperial College Press.
(3) Berber, S., Kwon, Y. K. and Tománek, D., “Unusually High Thermal Conductivity of Carbon Nanotubes”, *Phys. Rev. Lett.*, Vol.84, No.20 (2005), pp.4613-4616.
(4) Perebeinos, V., Tersoff, J. and Avouris, P., “Electron-phonon Interaction and Transport in Semiconducting Carbon Nanotubes”, *Phys. Rev. Lett.*, Vol.94, No.8 (2005), 086802.
(5) Fujii, M., Zhang, X., Xie, H., Ago, H., Takahashi, K., Ikuta, T., et al., “Measuring the Thermal Conductivity of a Single Carbon Nanotube”, *Phys. Rev. Lett.*, Vol.95, No.6 (2005), 065502.
(6) Ebbesen, T. W., Lezec, H. J., Hiura, H., Bennett, J. W., Ghaemi, H. F. and Thio, T., “Electrical Conductivity of Individual Carbon Nanotubes”, *Nature*, Vol.382, No.6586 (1996), pp.54-56.
(7) Czerw, R., Terrones, M., Charlier, J. -C., Blasé, X., Foley, B., Kamalakaran, R., et al., “Identification of Electron Donor States in N-doped Carbon Nanotubes”, *Nano Lett.*, Vol.1, No.9 (2001), pp.457-460.
(8) Li, Y., Kim, W., Zhang, Y., Rolandi, M., Wang, D., Dai, H., “Growth of Single-walled Carbon Nanotubes from Discrete Catalytic Nanoparticles of Various Sizes”, *J. Phys. Chem. B*, Vol.105, No.46 (2001), pp.11424-11431.
(9) Cheung, C. L., Kurtz, A., Park, H. and Lieber, C. M., “Diameter-controlled Synthesis of Carbon Nanotubes”, *J. Phys. Chem. B*, Vol.106, No.10 (2002), pp.2429-2433.
(10) Awano, Y., Sato, S., Kondo, D., Ohfuti, M., Kawabata, A., Nihei, M., et al., “Carbon Nanotube via Interconnect Technologies: Size-classified Catalyst Nanoparticles and Low-resistance Ohmic Contact Formation”, *Phys. Status Solidi A*, Vol.203, No.14 (2006), pp.3611-3616.
(11) Zhang, M., Atkinson, K. R. and Baughman, R. H., “Multifunctional Carbon Nanotube Yarns by Downsizing an Ancient Technology”, *Science*,

Vol.306, No.5700 (2004), pp.1358-1361.
(12) Fan, S., Chapline, M. G., Franklin, N. R., Tombler, T. W., Cassell, A. M. and Dai, H., "Self-oriented Regular Arrays of Carbon Nanotubes and Their Field Emission Properties", *Science*, Vol.283, No.5401 (1999), pp.512-514.
(13) Chhowalla, M., Teo, K. B. K., Ducati, C., Rupesinghe, N. L., Amaratunga, G. A. J., Ferrari, A. C., et al., "Growth Process Conditions of Vertically Aligned Carbon Nanotubes Using Plasma Enhanced Chemical Vapor Deposition", *J. Appl. Phys.*, Vol.90, No.10 (2001), pp.5308-5317.
(14) Hata, K., Futaba, D. N., Mizuno, K., Namai, T., Yumura, M. and Iijima, S., "Water-assisted Highly Efficient Synthesis of Impurity-free Single-walled Carbon Nanotubes", *Science*, Vol.306, No.5700 (2004), pp.1362-1364.
(15) Akoshima, M., Hata, K., Futaba, D. N., Baba, T., Kato, H. and Yumura, M., "Thermal Diffusivity of Single-walled Carbon Nanotube Forest Measured by Laser Flash Method", *Jpn. J. Appl. Phys.*, Vol.48, No.5 (2009), 05EC07.
(16) Wang, X. B., Liu, Y. Q., Yu, G., Xu, C. Y., Zhang, J. B. and Zhu, D. B., "Anisotropic Electrical Transport Properties of Aligned Carbon Nanotube Films", *J. Phys. Chem. B*, Vol.105, No.39 (2001), pp.9422-9425.
(17) Futaba, D. N., Hata, K., Yamada, T., Hiraoka, T., Hayamizu, Y., Kakudate, Y., et al., "Shape-engineerable and Highly Densely Packed Single-walled Carbon Nanotubes and Their Application as Super-capacitor Electrodes", *Nat. Mater.*, Vol.5, No.12 (2006), pp.987-994.
(18) Gunjishima, I., Inoue, T., Yamamuro, S., Sumiyama, K. and Okamoto, A., "Growth of Vertically Aligned Carbon Nanotubes from Highly Active Fe-Ti-O Nanoparticles Prepared by Liquid-phase Synthesis", *Jpn. J. Appl. Phys.*, Vol.46, No.6A (2007), pp.3700-3703.
(19) Gunjishima, I., Inoue, T., Yamamuro, S., Sumiyama, K. and Okamoto, A., "Synthesis of Vertically Aligned, Double-walled Carbon Nanotubes from Highly Active Fe-V-O Nanoparticles", *Carbon*, Vol.45, No.6 (2007), pp.1193-1199.
(20) Gunjishima, I., Inoue, T. and Okamoto, A., "Improved Diameter Control of Carbon Nanotubes Using Fe-V-O Nanoparticles as the Catalyst", *Jpn. J. Appl. Phys.*, Vol.47, No.4 (2008), pp.2313-2316.
(21) Inoue, T., Gunjishima, I. and Okamoto, A., "Synthesis of Diameter-controlled Carbon Nanotubes Using Centrifugally Classified Nanoparticle Catalysts", *Carbon*, Vol.45, No.11 (2007), pp.2164-2170.
(22) Gunjishima, I., Inoue, T. and Okamoto, A., "Growth of Diameter-controlled Carbon Nanotubes from Fe-V-O Nanoparticles Size-classified by Ligand-exchanged Fractional Precipitation", *Langmuir*, Vol.24, No.6 (2008), pp.2407-2411.
(23) Okamoto, A., Gunjishima, I., Inoue, T., Akoshima, M., Miyagawa, H., Nakano, T., et al., "Thermal and Electrical Conduction Properties of Vertically Aligned Carbon Nanotubes Produced by Water-assisted Chemical Vapor Deposition", *Carbon*, Vol.49, No.1 (2011), pp.294-298.
(24) Ohta, R., Shimazu, T., Siry, M., Gunjishima, I., Nishikawa, K., Oshima, H. and Okamoto, A., "Alignment-retainable Nitrogenation of Cylindrical Carbon Nanotubes by Thermal Reaction with Ammonia Following UV Oxidation: Chemical Alteration Effects on Electrical Conductivity", *Chem. Commun.*, Vol.47, No.13 (2011), pp.3873-3875.
(25) Yamamuro, S., Ando, T., Sumiyama, K., Uchida, T. and Kojima, I., "Monodisperse Metallic Iron Nanoparticles Synthesized from Noncarbonyl Complex", *Jpn. J. Appl. Phys.*, Vol.43, No.7A (2004), pp.4458-4459.
(26) Fukuoka, A., Araki, H., Sakamoto, Y., Sugimoto, N., Tsukada, H., Kumai, Y., et al., "Template Synthesis of Nanoparticle Arrays of Gold and Platinum in Mesoporous Silica Films", *Nano Lett.* Vol.2, No.7 (2002), pp.793-795.
(27) Gunjishima, I., Inoue, T. and Okamoto, A., "In Situ Optical Imaging of Carbon Nanotube Growth", *Jpn. J. Appl. Phys.*, Vol.46, No.5A (2007), pp.3149-3151.
(28) Gunjishima, I., Inoue, T. and Okamoto, A., "In Situ Growth Rate Control of Carbon Nanotubes by Optical Imaging Method", *Appl. Phys. Lett.*, Vol.91, No.19 (2006), 193102.
(29) Fu, Q., Huang, S. M. and Liu, J., "Chemical Vapor Depositions of Single-walled Carbon Nanotubes Catalyzed by Uniform Fe_2O_3 Nanoclusters Synthesized Using Diblock Copolymer Micelles", *J. Phys. Chem. B*, Vol.108, No.20 (2004), pp.6124-6129.
(30) Choi, H. C., Kim, W., Wang, D. W. and Dai, H. J., "Delivery of Catalytic Metal Species onto Surfaces with Dendrimer Carriers for the Synthesis of Carbon Nanotubes with Narrow Diameter Distribution", *J. Phys. Chem. B*, Vol.106, No.48 (2002), pp.12361-12365.
(31) Kobayashi, Y., Nakashima, H., Takagi, D. and Homma, Y., "CVD Growth of Single-walled Carbon Nanotubes Using Size-controlled Nanoparticle Catalyst", *Thin Solid Films*, Vols.464-465 (2004), pp.286-289.
(32) Sato, S., Kawabata, A., Kondo, D., Nihei, M. and Awano, Y., "Carbon Nanotube Growth from Titanium-cobalt Bimetallic Particles as a Catalyst", *Chem. Phys. Lett.*, Vol.402, No.1-3 (2005) pp.149-154.
(33) Sato, S., Kawabata, A., Nihei, M. and Awano, Y., "Growth of Diameter-controlled Carbon Nanotubes Using Monodisperse Nickel Nanoparticles Obtained with a Differential Mobility Analyzer", *Chem. Phys. Lett.*, Vol.382, No.3 (2003), pp.361-366.
(34) Akoshima, M. and Baba, T., "Thermal Diffusivity Measurements of Candidate Reference Materials by

the Laser Flash Method", *Int. J. Thermophys.*, Vol.26, No.1 (2005), pp.151-163.
(35) de Heer, W. A., Bacsa, W. S., Châtelain, A., Gerfin, T., Humphrey-Baker, R., Forro, L., et al., "Aligned Carbon Nanotube Films: Production and Optical and Electronic Properties", *Science*, Vol.268, No.5212 (1995), pp.845-847.
(36) Mott, N. F., "Conduction in Non-crystalline Materials III. Localized States in a Pseudogap and Near Extremities of Conduction and Valence Bands", *Philos. Mag.*, Vol.19, No.160 (1969), pp.835-852.
(37) Yosida, Y. and Oguro, T., "Variable Range Hopping Conduction in Multiwalled Carbon Nanotubes", *J. Appl. Phys.*, Vol.83, No.9 (1998), pp.4985-4987.
(38) Shen, J. Y., Chen, Z. J., Wang, N. L., Li, W. J. and Chen, L. J., "Electrical Properties of a Single Microcoiled Carbon Fiber", *Appl. Phys. Lett.*, Vol.89, No.15 (2006), 153132.
(39) Kaji, S., Oomi, G., Tomioka, Y. and Tokura, Y., "Effect of Pressure on the Electrical Resistivity of Double Perovskite $Sr_2FeW_{0.75}Mo_{0.25}O_6$", *Physica B*, Vol.359-361 (2005), pp.1327-1329.
(40) Okpalugo, T. I. T., Papakonstantinou, P., Murphy, H., McLaughlin, J. A. D. and Brown, N. M. D., "High Resolution XPS Characterization of Chemical Functionalised MWCNTs and SWCNTs", *Carbon*, Vol.43, No.1 (2005), pp.153-161.
(41) Ripalda, J. M., Román, E., Díaz, N., Galán, L., Montero, I., Comelli, G., Baraldi, A., Lizzit, S., Goldoni, A. and Paolucci, G., "Correlation of X-ray Absorption and X-ray Photoemission Spectroscopies in Amorphous Carbon Nitride", *Phys. Rev. B*, Vol.60, No.6 (1999), pp.R3705-R3708.
(42) Casanovas, J., Ricart, J. M., Rubio, J., Illas, F. and Jiménez-Mateos, J. M., "Origin of the Large N 1s Binding Energy in X-ray Photoelectron Spectra of Calcined Carbonaceous Materials", *J. Am. Chem. Soc.*, Vol.118, No.34 (1996), pp 8071-8076.
(43) Mawhinney, D. B., Naumenko, V., Kuznetsova, A., Yates, J. T., Jr., Liu, J. and Smalley, R. E., "Infrared Spectral Evidence for the Etching of Carbon Nanotubes: Ozone Oxidation at 298 K", *J. Am. Chem. Soc.*, Vol.122, No.10 (2009), pp.2383-2384.
(44) Guo, Q., Xie, Y., Wang, X., Zhang, S., Hou, T. and Lv, S., "Synthesis of Carbon Nitride Nanotubes with the C_3N_4 Stoichiometry via a Benzene-thermal Process at Low Temperatures", *Chem. Commun.*, No.1 (2004), pp.26-27.
(45) Zhang, S. J., Krzysztof, K. K. K., Kinloch, I. A. and Windle, A. H., "Macroscopic Fibers of Well-aligned Carbon Nanotubes by Wet Spinning", *Small*, Vol.4, No.8 (2008), pp.1217-1222.
(46) Lee, D. H., Lee, W. J. and Kim, S. O., "Highly Efficient Vertical Growth of Wall-number-selected, N-doped Carbon Nanotube Arrays", *Nano Lett.*, Vol.9, No.4 (2009), pp.1427-1432.
(47) Terrones, M., Jorio, A., Endo, M., Rao, A. M., Kim, Y. A., Hayashi, T., Terrones, H., Charlier, J. C., Dresselhaus, G. and Dresselhaus, M. S., "New Direction in Nanotube Science", *Materials Today*, Vol.7, No.10 (2004), pp.30-45.
(48) Rao, C. V., Cabrera, C. R. and Ishikawa, Y., "In Search of the Active Site in Nitrogen-doped Carbon Nanotube Electrodes for the Oxygen Reduction Reaction", *J. Phys. Chem. Lett.*, Vol.1, No.18 (2010), pp.2622-2627.

Table 1 and Figs. 5-7
Reprinted from Carbon, Vol.49, No.1 (2011), pp.294-298, Okamoto, A., Gunjishima, I., Inoue, T., Akoshima, M., Miyagawa, H., Nakano, T., Baba, T., Tanemura, M. and Oomi, G., Thermal and Electrical Conduction Properties of Vertically Aligned Carbon Nanotubes Produced by Water-assisted Chemical Vapor Deposition, © 2011 Elsevier, with permission from Elsevier.

Figs. 8 and 9
Reprinted from Chem. Commun., Vol.47, No.13 (2011), pp.3873-3875, Ohta, R., Shimazu, T., Siry, M., Gunjishima, I., Nishikawa, K., Oshima, H. and Okamoto, A., Alignment-retainable Nitrogenation of Cylindrical Carbon Nanotubes by Thermal Reaction with Ammonia Following UV Oxidation: Chemical Alteration Effects on Electrical Conductivity, © 2011 RSC, with permission from the Royal Society of Chemistry.

Atsuto Okamoto
Research Fields:
- Surface and Coatings Technology
- Synthesis and Characterization of Nanocarbons

Academic Societies:
- The Japan Society of Applied Physics
- The Japanese Association for Crystal Growth
- The Carbon Society of Japan

Award:
- The 32nd National Conference on Crystal Growth Incentive Award, the Japanese Association for Crystal Growth, Japan, 2002

Itaru Gunjishima
Research Fields:
- Silicon Carbide
- Carbon Nanotube
- Nanoparticle

Academic Degree: Dr. Eng.
Academic Society:
- The Japan Society of Applied Physics

Takashi Inoue*

Research Field:
- Material Science

Academic Degree : Dr. Sci.

Academic Societies:
- The Chemical Society of Japan
- The Fullerenes, Nanotubes and Graphene Research Society

Award:
- CSJ Student Presentation Award 2004, the Chemical Society of Japan, 2004

Riichiro Ohta

Research Fields:
- Surface Finishing
- Synthesis of Carbon-based Nanomaterials

Academic Degree: Dr. Eng.

Academic Society:
- The Japan Society of Applied Physics

Koichi Nishikawa

Research Field:
- Materials Research for Semiconductor Devices

Academic Degree: Dr. Eng.

Academic Societies:
- The Japan Society of Applied Physics
- The Japanese Association for Crystal Growth
- The Japan Institute of Metals

*Retired from TCRDL

